

An FEM-BEM Interactive Coupling for Modeling Smart Structural Health Monitoring Systems

A. A. Shah

*Professor and Chairman, Department of Civil Engineering, Sarhad University of Science and Information Technology Peshawar, KPK, Pakistan
hod.civil@suit.edu.pk, drabidali@gmail.com*

O. Tariq

Lecturer, Department of Civil Engineering, Sarhad University of Science and Information Technology Peshawar, KPK, Pakistan

U. Amjad

Lecturer, Department of Civil Engineering, Iqra National University Peshawar, KPK, Pakistan

H. Afridi

Consulting Engineer, DECON Engineering Consultants Peshawar, KPK, Pakistan

Abstract

In this research modeling of piezo-electric smart structural health monitoring systems is presented. The work is aimed at determining the actuation effects being transferred from the actuators to the host and the resulting overall structural response. To obtain the amount of these actuations, the system of the host structure and an actuator has been modeled by using coupled finite element boundary element method in frequency domain. The host structure, which is assumed as an isotropic elastic solid region is modeled as a half space. The piezoelectric ceramic region is modeled by the 3-D finite element method, while the elastic half space with boundary element method. Finite element model of piezoelectric ceramic and boundary element model of the elastic half space are coupled together at their interface such that the vibrations of the piezo-actuator induce vibrations in the elastic half space. The numerical results show that high jump in magnitude of horizontal displacements at the corners of the actuator attached to the structure occurs, which is an indication of high stress concentration, of the shear stress type at the corners. The presented work is a step towards modeling of structural health monitoring systems.

Keywords

Actuators, Boundary Element, Finite Element, Piezoelectric, Smart Structure, Stress Concentration

1. Introduction

In recent years, structural health monitoring (SHM) has emerged as a concept in the broader field of investigation of smart structures (Noor, 2000; Staszewski *et al.*, 2004). Structural systems are usually described as smart when they are able to sense and adapt their response to changing operational or environmental conditions. Their development relies on the integration of sensors and actuators with the structure and on the combination with appropriate electronics, modeling and control algorithms. SHM

systems exploit such features to detect the occurrence and location of damage which may affect the performance and reliability of the structure. While conventional non-destructive inspection procedures investigate directly for damage at scheduled intervals applying the appropriate technique, in situ SHM systems are generally based on the real time comparison of the local or global response of the damaged structure with the known response of the undamaged one.

In piezoelectric structural usage and health monitoring systems, the monitoring is performed through a network of suitably arranged piezoelectric sensors, some physical variables and fields, such as strain, vibration, electrical conductivity and acoustic emission, which may be affected by the changes of material and geometrical conditions in proximity of the damaged area. This system has an advantage of the direct piezoelectric effect, which refers to the generation of an electric displacement field as a consequence of a mechanical load. As a result it is able to sense structural deformation and signal it through a variation of voltage or rate of variation of voltage (Chopra, 2002).

Piezoelectric materials are among the most widely used smart materials because of their reliability and sensitivity (Lin, 2011). Their common use as sensors/actuators in smart structures is also due to their fast response and low energy consumption (Deng and Wang, 2002). A piezoelectric actuator usually consists of two main components (Juuti *et al.*, 2005): a mechanical part, which is a flexible structure, and an electrical part, which is the piezoelectric material block. One of the important issues of using piezoelectric actuator is to improve their performance for a certain amount of piezoelectric material, which is the goal of piezoelectric actuator design. Since the mechanical part of flextensional actuators is actually a compliant mechanism, piezoelectric transducer (Li *et al.*, 2001) and thermal actuators (Yoon *et al.*, 2005) have been also designed using topology optimization technique. This topological design optimization was able to generate effective mechanical structure that greatly improved the performances of the piezoelectric actuator.

Piezoelectric actuator has been increasingly used in MEMS system due to its advantage of generality and flexibility. A flextensional actuator consists of a piezoceramic device, which can convert electrical energy into mechanical energy and vice versa, and a flexible mechanical structure, which can convert and amplify the output piezoceramic displacement in the desired direction and magnitude (Yoon *et al.*, 2004). A recent research in this area is optimizing the topology of the mechanical part while fixing the electrical part (Yoon and Sigmund, 2008). There have also been design optimization techniques developed for the electrical part of piezoelectric actuator. The placement and size of piezo-material was optimized (Main *et al.*, 1994). In a recent research, the distribution of piezoelectric material in the optical MEMS was optimized (Gabbert and Weber, 1999).

With reference to the research in (Mackerle, 1999), for modeling of sensors and actuators frequently boundary element method (BEM) based formulations have to be coupled with finite element method (FEM) formulations. Because each method performs better than the other in some domains or some parts of the same domain. Therefore, a combined approach could be both accurate and efficient for a large class of problems. For example, problems with high stress gradient regions could be modeled using BEM while FEM could be used for the rest of the structure. Zhang *et al.* (2003) analyzed the problem of a piezoelectric layer bonded to an elastic substrate, considering the full coupling between electrical and mechanical fields. Ali *et al.* (2004) developed an analytical model for constrained piezoelectric thin film sensors and applied the model to the analysis of the problem of detection of subsurface cracks (Ali *et al.*, 2005). An analytical solution for the coupled electromechanical dynamic behavior of a piezoelectric actuator bonded to an infinite orthotropic elastic medium has been developed by Huang and Sun (2006). The earlier efforts at integrating boundary elements and finite elements have been problematic and inefficient due to the unsymmetrical nature of the boundary element method. This process becomes even more cumbersome in a typical assembly process. When the different parts of a structure are modeled independently of each other in a sub-domain format, it is important to keep account of the fact that the nodes at the interfaces match exactly (Brebbia and Georgiou, 1979; Eberhardsteiner *et al.*, 1993; Jeans and Matthews, 1999).

This paper is concerned with the development of a three dimensional numerical model for the dynamic interaction of a piezoelectric ceramic bonded on the surface of a semi-infinite elastic domain. In this numerical technique finite element method is implemented for the modeling of the piezo-actuator and boundary element method for the semi-infinite isotropic elastic domain. The model considers dynamic

interaction of the two materials in frequency domain. This method is usually used to solve the problems which deal with sort of coupling or interaction of two media because both FEM and BEM are very powerful numerical tools the coupling of which have the advantage of modeling the complex piezoelectric materials economically and reliably.

2. FEM-BEM formulation and Coupling

Some material usually ceramics have a property called piezoelectricity (Gao et al., 2000). If stress is applied to such material, it will develop an electric moment proportional to the applied stress. This is the direct piezoelectric effect. Conversely, if it is placed in an electric field, a piezoelectric material changes its shape slightly. This is the inverse piezoelectric effect. Ceramics manufactured from lead zirconate/lead titanate group exhibit greater sensitivity and higher operating temperatures, relative to ceramics of other compositions, and "PZT" materials currently are the most widely used piezoelectric ceramics. Fig. 1 shows this property in a cylindrical piezoelectric material.

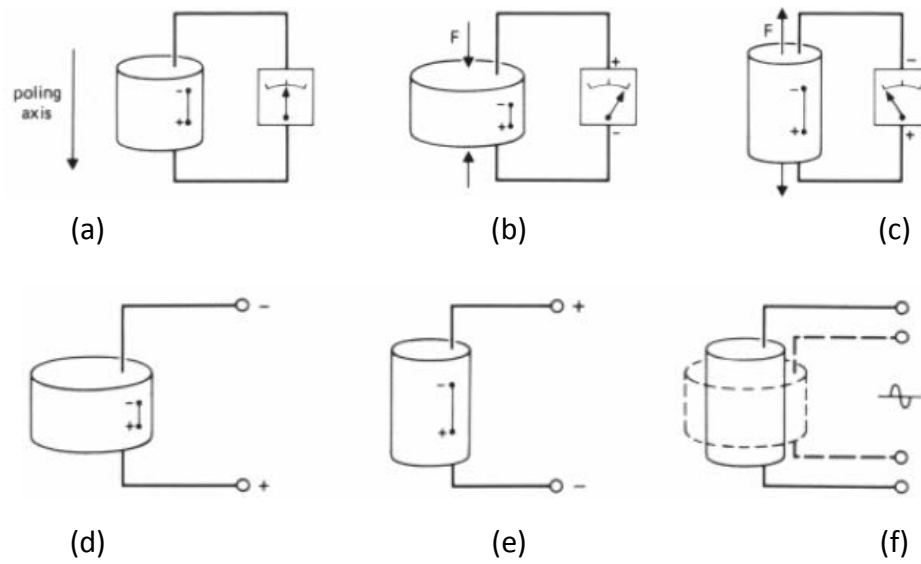


Figure 1: The Piezoelectric effect in a cylindrical body of piezoelectric ceramic (a) no load, (b) compressed, (c) stretched, (d) shorten, (e) lengthen, and (f) grow and shrink (Yang, 2005)

The constitutive equations of the piezoelectric materials are given by

$$\tau_{ij} = C_{ijkl} S_{kl} - e_{kij} E_k ; \quad (1)$$

$$D_i = e_{ikl} S_{kl} + \varepsilon_{ik} E_k ; \quad (2)$$

where C is the elasticity matrix for constant strain, ε is the matrix of dielectric constants for constant mechanical strain, e is matrix of piezoelectric constants, and τ , S , E and D are vectors of stress, strain, electric field and electric displacement, respectively. In the finite element formulation, the displacement

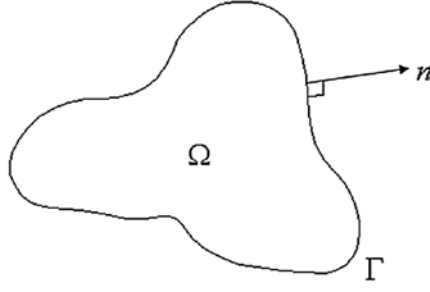


Figure 3: The domain Ω with surface Γ and outward unit normal

Eq. (7) shows the displacement fundamental solution for an elastic, homogeneous and isotropic continuum in frequency domains for infinite medium.

$$U_i(x, y) = \frac{1}{4\pi\mu} \left[\frac{e^{ik_r r}}{r} + \frac{1}{k_T^2} \left\{ \frac{e^{ik_r r}}{r} - \frac{e^{ik_l r}}{r} \right\} \right]; \quad (7)$$

where k_s, k_p are shear wave number and pressure wave number, respectively and r is the distance between the source point y and the field point x .

For BEM integral formulation in frequency domain, Betti Reciprocal Theorem is considered to formulate the following relationship.

$$\int_{\Gamma} P_i^1(x, \omega) U_i^2(x, \omega) d\Gamma + \int_{\Omega} \rho B_i^1(x, \omega) U_i^2(x, \omega) d\Omega = \int_{\Gamma} P_i^2(x, \omega) U_i^1(x, \omega) d\Gamma + \int_{\Omega} \rho B_i^2(x, \omega) U_i^1(x, \omega) d\Omega; \quad (8)$$

Similarly, the BEM formulation for a single collocation node with the coordinate x is written as:

$$C(x) U_i(\omega) + \sum_{j=1}^{NE} \left\{ \int_{\Gamma_j} P^*(x_i, \omega; y) \Phi_j(y) d\Gamma_j \right\} U_i(\omega) = \sum_{j=1}^{NE} \left\{ \int_{\Gamma_j} U^*(x_i, \omega; y) \Phi_j(y) d\Gamma_j \right\} P_j(\omega); \quad (9)$$

where NE is the number of boundary elements in the domain. $U_i(\omega)$ are the complex amplitude of displacement at x_i . The N matrix equations for each of the collocation nodes in the BE domain may all be assembled into a single, global matrix equation for the entire domain (Brebbia, 2006) as

$$(\hat{C} + \hat{H})U = GP; \quad (10)$$

Eq. (10) can be simplified as expressed by Eq. (11):

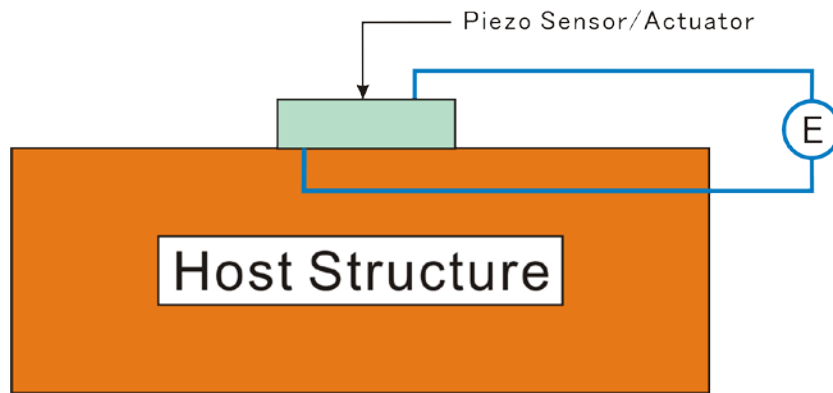
$$HU = GP; \quad (11)$$

considering that

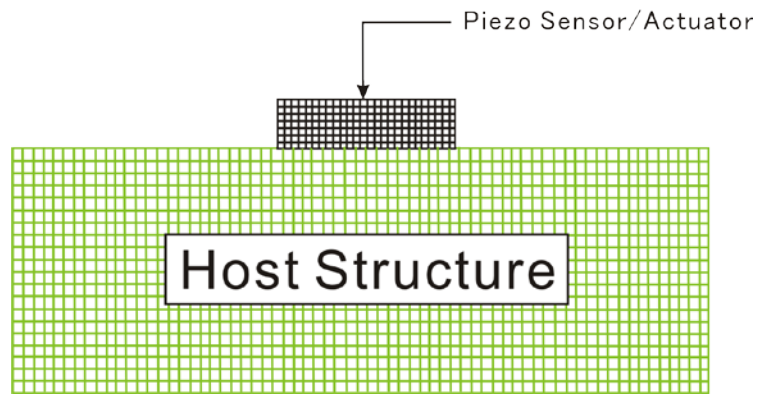
$$H = (\hat{C} + \hat{H}); \quad (12)$$

Eq. (12) is usually referred to as the basic formulation for boundary element system in matrix form, before any boundary conditions are taken into account.

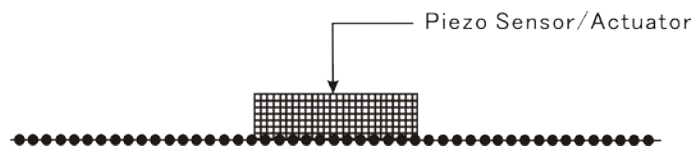
Coupling of BEM and FEM is established to develop a combine relationship, which is applied to compute the actuation effect of a piezo-actuator on a body. FEM-BEM method is very effective when the size of the piezo-device and the host structure are very different as shown in Fig. 9 (a) for the two dimensional case. From Fig. 9 (b) it is clearly observed that for such a problem the required elements number becomes so high that does not justify meshing the whole domain and hence using FEM in the first place. In Fig. 9 (c) finite element model of piezo-actuator and boundary element model of the host structure are coupled together. Fig. 10 shows the FEM and BEM regions, which were combine together and analyze through the system of equations, as discussed above, using FE and BE approaches.



(a)



(b)



(c)

Figure 9: Piezo-device and the host structures (a) piezo-device attached on the surface of the host structure, (b) piezo-device and the host structure modeled by FEM, and (c) piezo-device and the host structure modeled by FEM-BEM

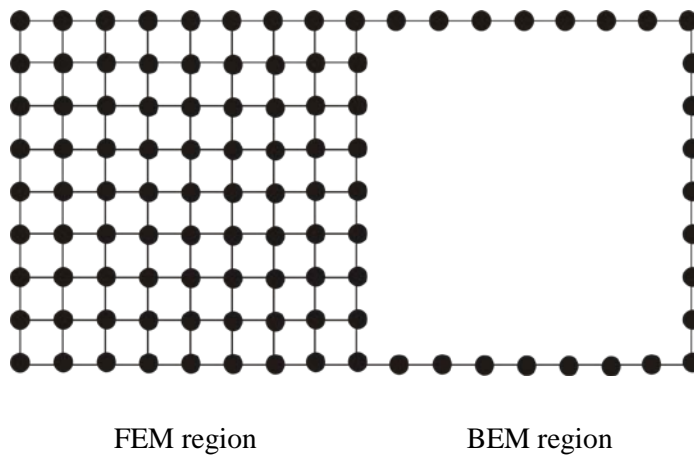


Figure 10: FEM-BEM region

In order to consider this region similar to a finite element region, the Eq. (12) is modified as:

$$G^{-1}HU = P; \quad (13)$$

Next, considering M as a tensor which transforms the vector of nodal tractions of the whole system to that of nodal forces and multiplying both sides of Eq. (24) by M , we obtain the following equation:

$$MG^{-1}HU = MP; \quad (14)$$

or simply

$$K'U = f; \quad (15)$$

where $K' = MG^{-1}H$ and f is the vector of nodal forces. Eq. (15) is similar to the finite element system of equations and thus boundary element region can be assumed as one super finite element and fed into the existing finite element system of equations.

3. Numerical Results

3.1 Surface-bonded PZT-4 actuator on steel half-space

In this example a $6 \times 6 \times 4 \text{ mm}$ piezoelectric patch of the transversely isotropic PZT4, working as a piezoelectric actuator is attached on the surface of a steel medium as shown in Fig. 13.

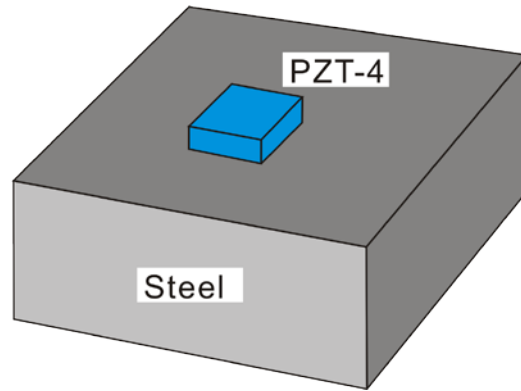


Figure 13: Surface bonded piezo-actuator on the steel medium

The poling direction of the actuator is along its thickness. A voltage (V) between the upper and the lower electrodes of the actuator is applied which results in an electric field with frequency of f along the poling direction of piezo-actuator. The medium is assumed as a half-space and it has been modeled by 298 boundary elements as in Fig. 14.

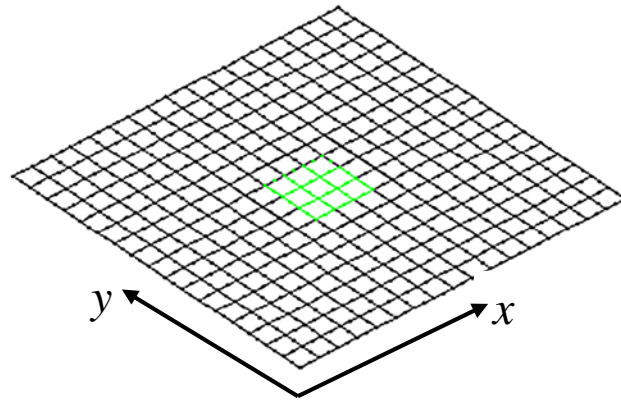


Figure 14: BEM half-space mesh to model steel domain

The piezo-actuator has been modeled by three and two elements in the plate's length direction and thickness direction respectively and it is placed at the middle of the half space mesh as indicated with green color in Fig. 14. Fig. 15 shows the FEM mesh to model the piezo-actuator using 9 finite elements.

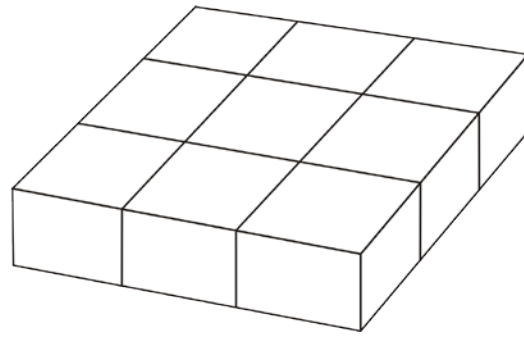


Figure 15: FEM mesh to model piezo-actuator

The nonzero elastic, piezoelectric and dielectric constants of PZT4 (Rouquette *et al.*, 2004) are:

$$\begin{array}{lll}
 C_{11} = C_{22} = 139 \text{ GPa} & & \\
 C_{12} = 77.8 \text{ GPa} & & \\
 C_{13} = C_{23} = 74.3 \text{ GPa} & e_{13} = e_{23} = -5.2 \text{ C/m}^2 & \varepsilon_{11} = \varepsilon_{22} = 13.06 \times 10^{-9} \text{ F/m} \\
 C_{33} = 115 \text{ GPa} & e_{33} = 15.1 \text{ C/m}^2 & \varepsilon_{33} = 11.51 \times 10^{-9} \text{ F/m} \\
 C_{44} = 30 \text{ GPa} & e_{52} = e_{61} = 12.7 \text{ C/m}^2 & \rho = 7800 \text{ kg/m}^3 \\
 C_{55} = C_{66} = 25.6 \text{ GPa} & &
 \end{array}$$

The host structure on the other hand is made of steel with the Young modulus of $E = 0.2 \times 10^{11} \text{ kg/m}^2$ and Poisson ratio of $\nu = 0.29$ or the pressure wave velocity of $C_p = 5900 \text{ m/s}$ and shear wave velocity of $C_s = 3200 \text{ m/s}$ and density of $\rho = 7900 \text{ kg/m}^3$. The piezo-actuator is connected to harmonic electric potential of $V = 300\sqrt{2} \text{ Exp}(5024000 \text{ it})$.

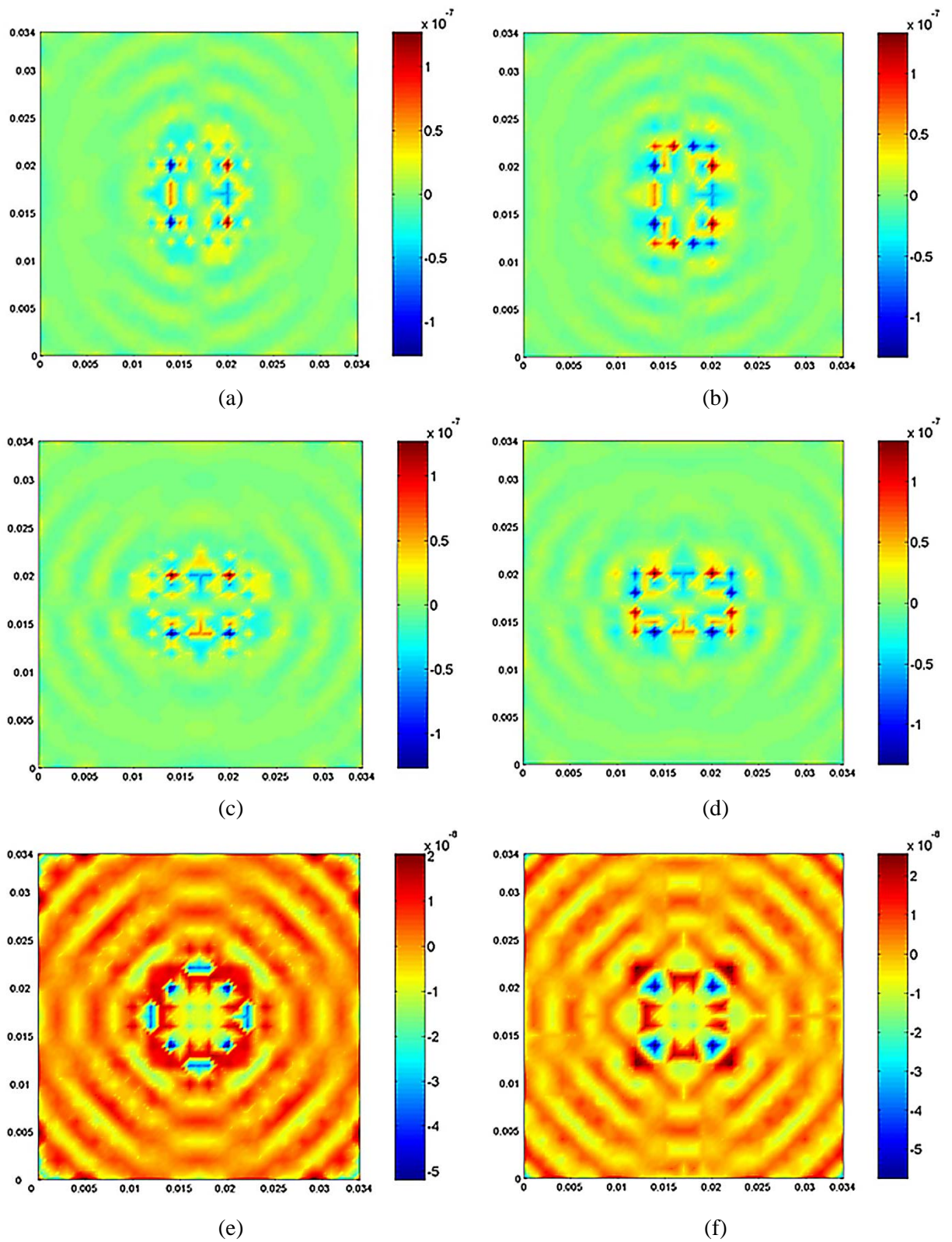
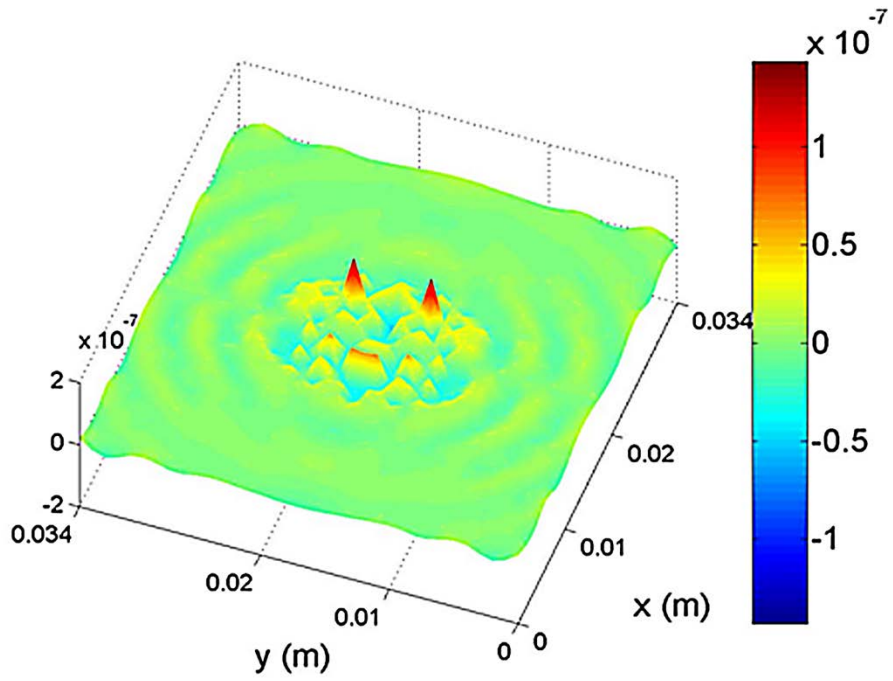
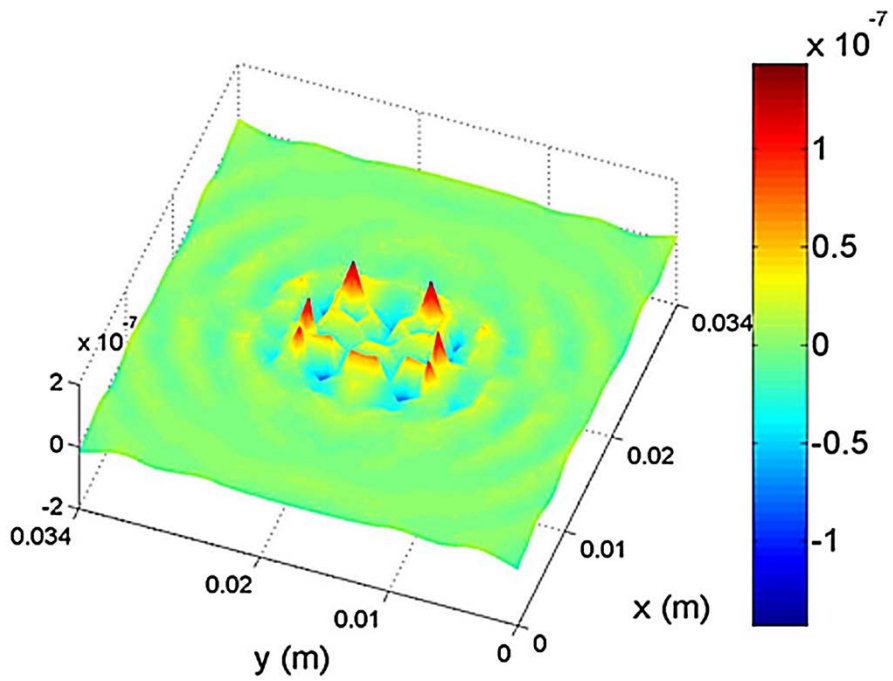


Figure 16: Displacement in plate with 4mm thickness (a) real part at x direction, (b) imaginary part at x direction, (c) real part at y direction, (d) imaginary part at y direction, (e) real part at z direction, and (f) imaginary part at z direction

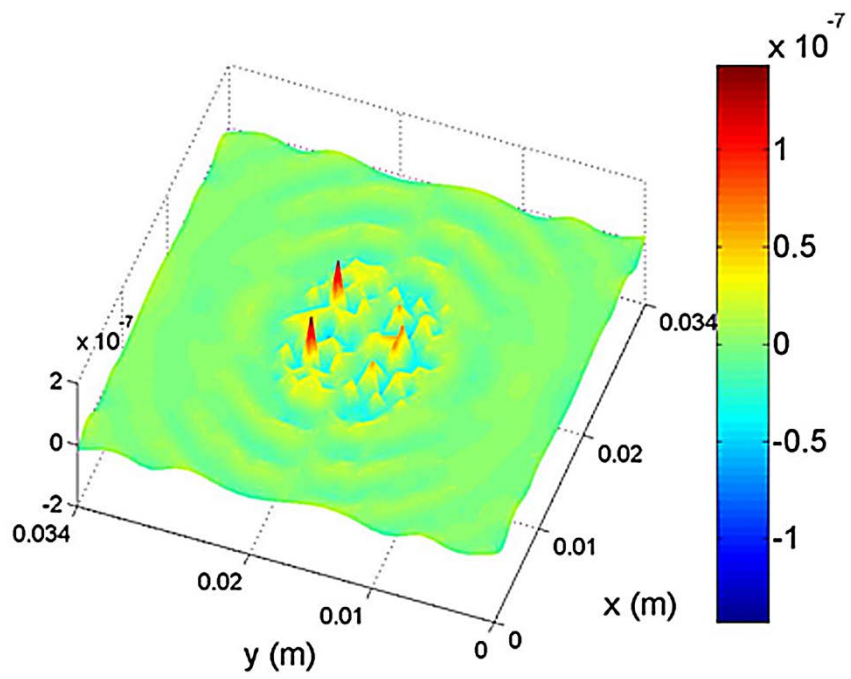


(a)

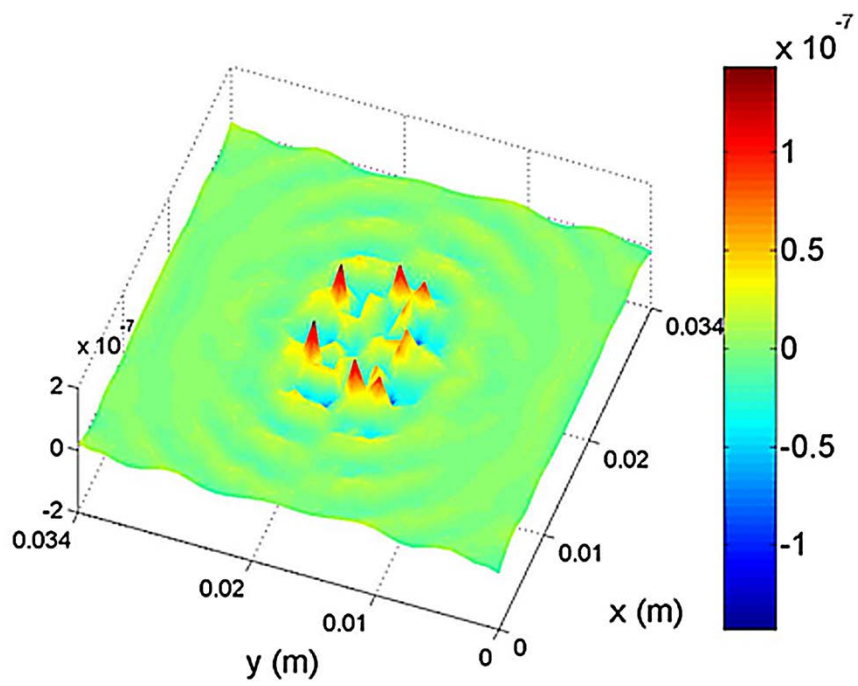


(b)

Figure 17: Displacement in x direction (a) real part, and (b) imaginary part

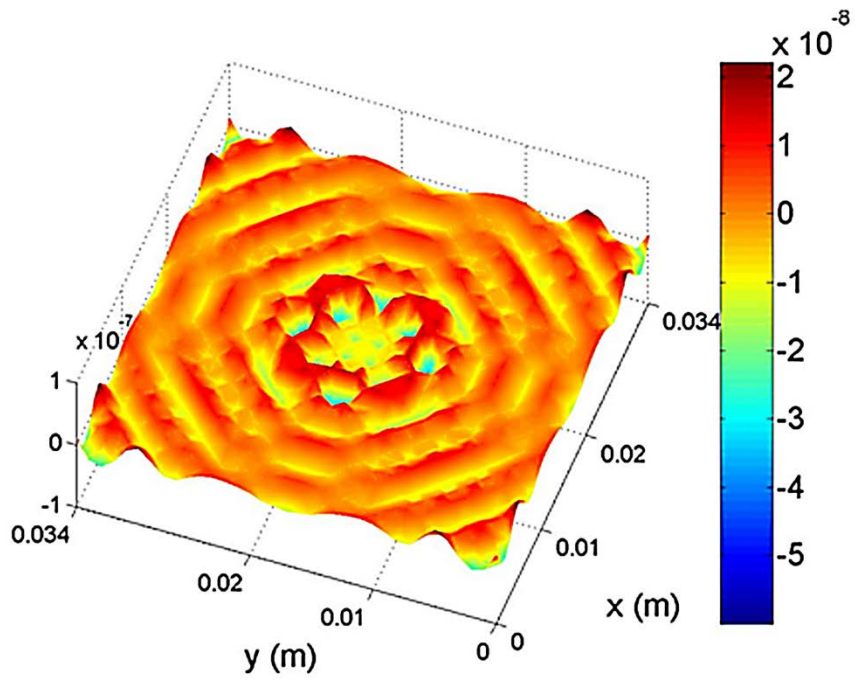


(a)

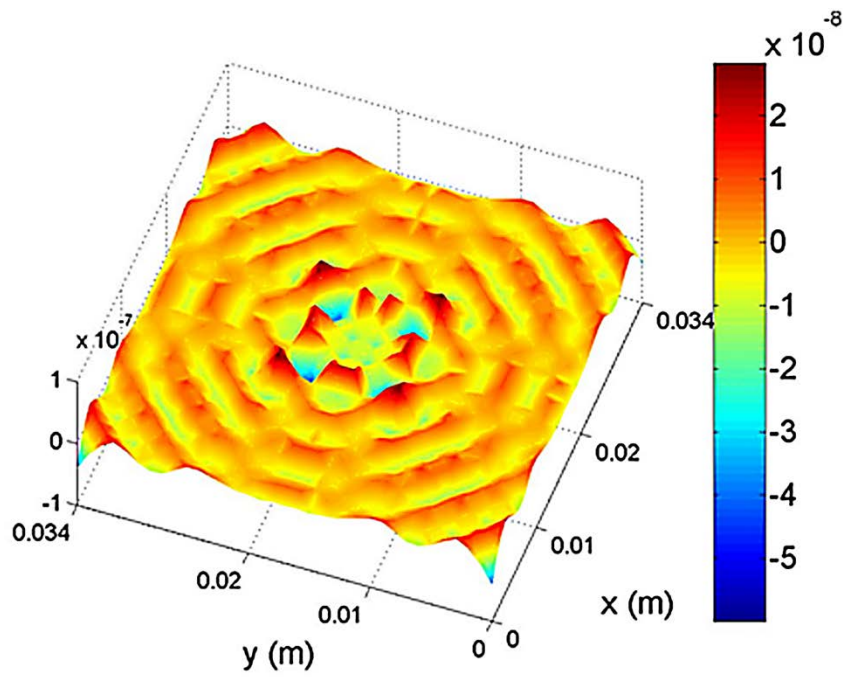


(b)

Figure 18: Displacement in y direction (a) real part, and (b) imaginary part



(a)



(b)

Figure 19: Displacement in z direction (a) real part, and (b) imaginary part

3.2 Surface-bonded PZT-5H actuator on steel (circular half-space)

In this example a $6 \times 6 \times 4 \text{ mm}$ piezoelectric patch of the transversely isotropic PZT-5H, working as a piezoelectric actuator is attached on the surface of a steel medium. The poling direction of the actuator is along its thickness. A voltage (V) between the upper and the lower electrodes of the actuator is applied which results in an electric field with frequency of f along the poling direction of piezo-actuator. The medium is assumed as a circular half-space and it is modeled by 489 boundary elements. The piezo-actuator has been modeled by nine finite elements, three elements in the length direction and one element in the thickness direction. The material properties of the PZT-5H (Liu *et al.*, 2000) are as follows: Elastic, piezoelectric and dielectric constants of PZT-5H

$$C_{11} = C_{22} = 126 \text{ GPa}$$

$$C_{12} = 79.5 \text{ GPa}$$

$$C_{13} = C_{23} = 84.1 \text{ GPa}$$

$$C_{33} = 126 \text{ GPa}$$

$$C_{44} = 23.3 \text{ GPa}$$

$$C_{55} = C_{66} = 23 \text{ GPa}$$

$$e_{13} = e_{23} = -6.5 \text{ C/m}^2$$

$$e_{33} = 23.3 \text{ C/m}^2$$

$$e_{52} = e_{61} = 17 \text{ C/m}^2$$

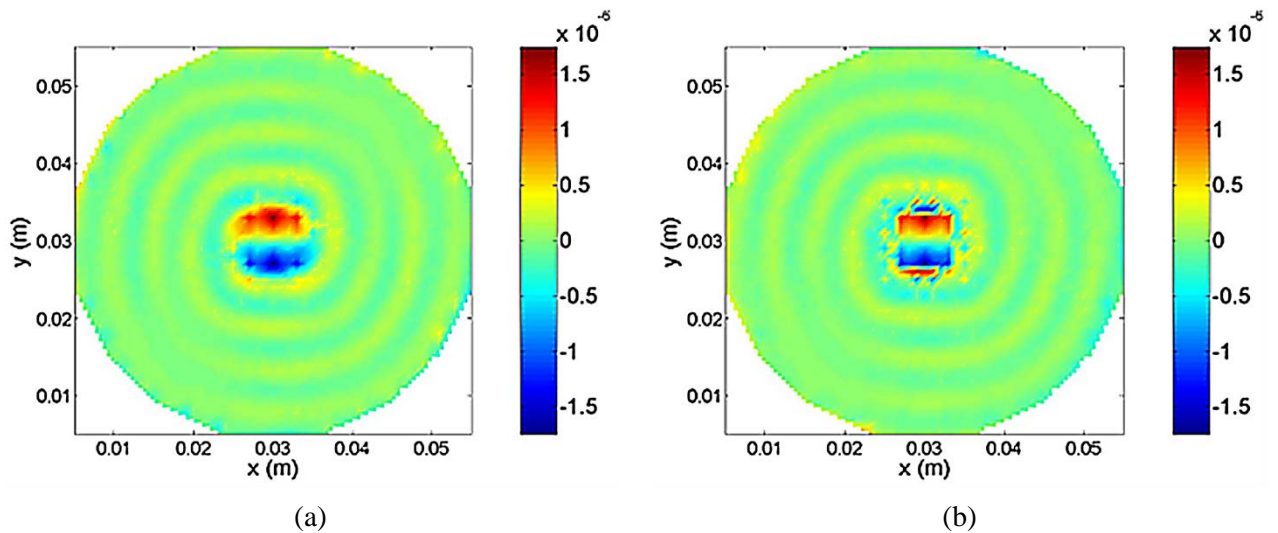
$$\epsilon_{11} = \epsilon_{22} = 1.503 \times 10^{-8} \text{ F/m}$$

$$\epsilon_{33} = 1.3 \times 10^{-8} \text{ F/m}$$

$$\rho = 7800 \text{ kg/m}^3$$

The second medium is made of steel with the Young modulus of $E = 0.2 \times 10^{12} \text{ GPa}$, and Poisson's ratio of $\nu = 0.29$ and density of $\rho = 7900 \text{ kg/m}^3$. The piezo-actuator is connected to the time harmonic electric potential of 1 kV and frequency of vibration of 590 kHz. Distribution of induced displacement field in horizontal and vertical directions on the surface of the circular half space steel medium are shown in Fig. 20.

In this example, since the BEM half space is modeled by circular area, the wave propagation is circular. Unlike the previous example, which shows that although the actuator is in rectangular shape but the wave propagation becomes circular when it takes distance from the actuator. Fig. 20 shows high values of displacements on the half space at the corner of actuator.



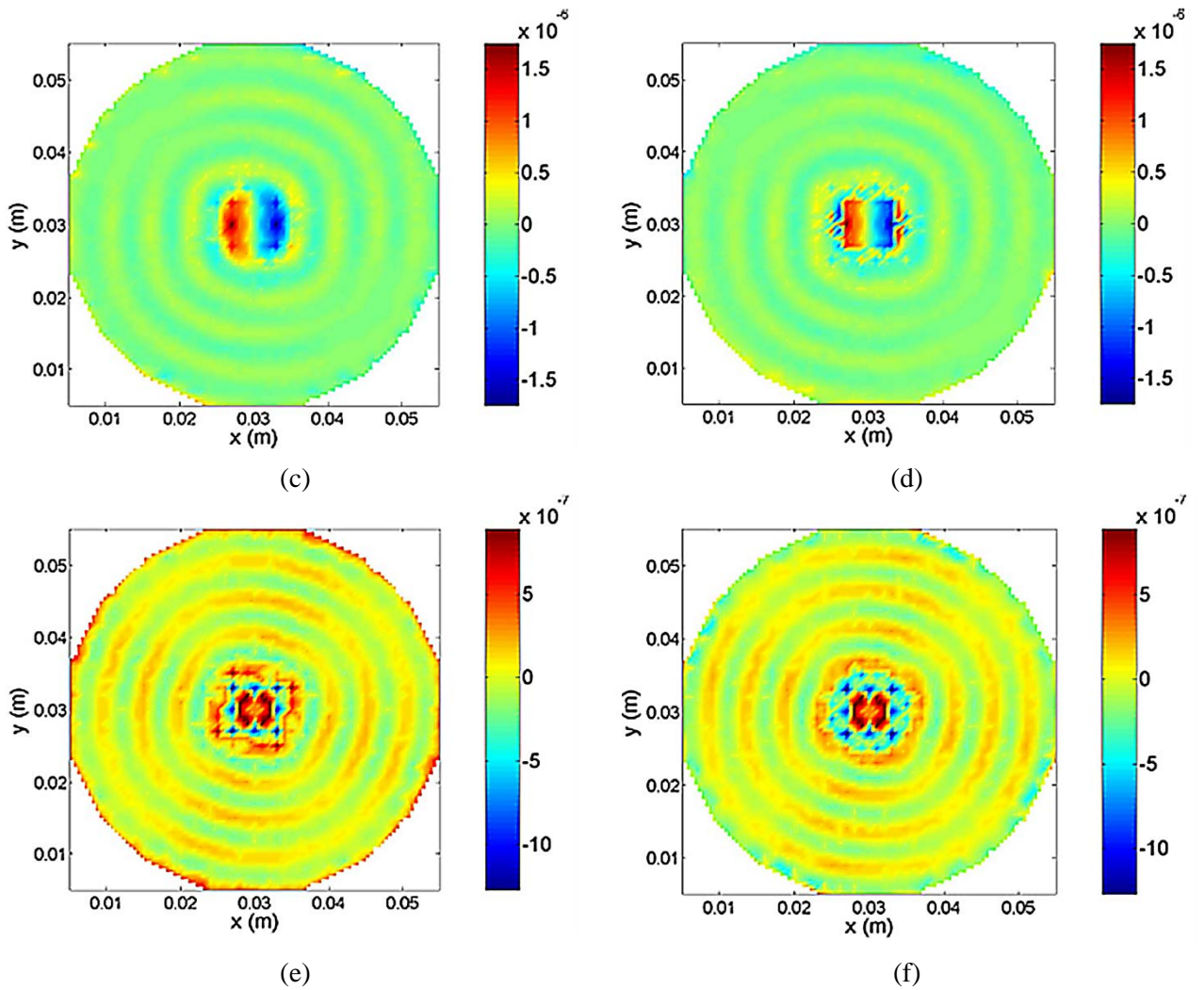


Figure 20: Displacement in plate with 4mm thickness (a) real part at x direction, (b) imaginary part at x direction, (c) real part at y direction, (d) imaginary part at y direction, (e) real part at z direction, and (f) imaginary part at z direction

4. Conclusions

In this research the coupling of finite element and boundary element for the interaction of a piezoelectric material and an isotropic elastic solid in frequency domain has been performed successfully. The results of this numerical modeling show high jumps in horizontal displacements of the half-space at the corners of the interface between the actuator and the elastic solid medium, which show that the high stress concentration occurs at the corners. The results further indicate that the displacement field induced by a piezo-actuator depends on the thickness of the actuator and for the thicker actuator we have smaller values of displacement induced in the host structure. The presented work will serve as a useful step towards modeling of structural health monitoring systems.

Acknowledgements The first author thankfully acknowledges the support provided by the Sarhad University of Science and Information Technology Peshawar for conducting this research.

References

- Noor, A.K. (2000). "Structures Technology for Future Aerospace Systems". *Progress in Astronautics and Aeronautics*, Vol. 188, American Institute of Aeronautics and Astronautics.
- Staszewski, W.C., Boller, C. and Tomlison, G.R. (2004). Health Monitoring of Aerospace Structures, *Smart Sensor Technologies and Signal Processing*, (Eds.), John Wiley & Sons Ltd.
- Chopra, I. (2002). "Review of state of art of smart structures and integrated systems". *Am. Inst. Aeronaut. Astronaut. J.*, Vol. 40, No. 11, pp 2145–2187.
- Lin, S. I. E. (2011). "The theoretical and experimental studies of a circular multi-layered annular piezoelectric actuator". *Sensors and Actuators A: Physical*, Vol. 165, pp 280–287.
- Deng, Q. L., and Wang, Z. Q. (2002). "Analysis of piezoelectric materials with an elliptical hole". *Acta Mech. Sinica*, Vol. 34, No. 1, pp 109–114.
- Juuti, J., Kord, K., Lonnakko, R., Moilanen, V.-P., and Leppävuori, S. (2005). "Mechanically amplified large displacement piezoelectric actuators". *Sensors and Actuators A*, Vol. 120, pp 225–231.
- Li, X., Vartuli, J.S., Milius, D.L., Aksay, I.A., Shih, W.Y., and Shih, W.-H. (2001). "Electromechanical properties of a ceramic d_{31} -gradient flextensional actuator". *J. Am. Ceram. Soc.*, Vol. 84, pp 996–1003.
- Yoon, C.-B., Lee, S.-M., Lee, S.-H., and Kim, H.-E. (2005). "PZN-PZT flextensional actuator by co-extrusion process". *Sensors and Actuators A*, Vol. 119, pp 221–227.
- Yoon, C.-B., Lee, S.-H., Seo, S.-B. and Kim, H.-E. (2004). "PZN-PZT flextensional actuators with conducting PZN-PZT/Ag layer by co-firing method". *J. Am. Ceram. Soc.*, Vol. 87, No. 9, pp 1663–1668.
- Yoon, G.H. and Sigmund, O. (2008). "A monolithic approach for topology optimization of electrostatically actuated devices". *Comput. Meth. Appl. Mech. Engrg.*, Vol. 97, pp 4062–4075.
- Main, J., Garcia, E., and Howard, D. (1994). "Optimal placement and sizing of paired piezoactuators in beams and plates". *Smart Material and Structure*, Vol. 3, pp 373–381.
- Gabbert, U., and Weber, C.-T. (1999). "Optimization of piezoelectric material distribution in smart structures". *Proceedings of SPIE- The International Society for Optical Engineering*, Vol. 3667, pp 13–22.
- Gao, F., Shen, Y. and Li, L. (2000). "Optimal design of piezoelectric actuators for plate vibro acoustic control using genetic algorithms with immune diversity". *Smart Mater. Struct.*, Vol. 9, pp 485–491.
- Mackerle, J. (1999). "Sensors and actuators: finite element and boundary element analyses and simulations". *A bibliography (1997–1998), Finite Elements Anal. Des.*, Vol. 33, pp 209–220.
- Zhang, J., Zhang, B. and Fan, J. (2003). "A coupled electromechanical analysis of piezoelectric layer bonded to an elastic substrate: Part I. Development of governing equations". *Int. J. Solids Struct.*, Vol. 40, pp 6781–6797.
- Ali, R., Mahapatra, D. R. and Gopalakrishnan, S. (2004). "An analytical model of constrained piezoelectric thin film sensors". *Sensors Actuators A*, Vol. 116, pp 424–437.
- Ali, R., Mahapatra, D. R. and Gopalakrishnan, S. (2005). "Constrained piezoelectric thin film for sensing of subsurface cracks". *Smart Mater. Struct.*, Vol. 14, pp 376–386.
- Huang, G.L. and Sun, C.T. (2006). "The dynamic behavior of a piezoelectric actuator bonded to an anisotropic elastic medium". *Int. J. Solids Struct.*, Vol. 43, pp 1291–1307.
- Brebbia, C. A. and Georgiou, P. (1979). "Combination of boundary and finite elements in elastostatics". *Applied Mathematical Modeling*, Vol. 3, pp 212–220.
- Eberhardsteiner, J., Mang, H.A. and Torzicky, P. (1993). "Three dimensional elasto-plastic BE-FE stress analysis of the excavation of a tunnel bifurcation on the basis of a substructuring technique". *Advances in Boundary Element Techniques*, Springer: Berlin, 103–128.
- Jeans, R.A. and Matthews, I.C. (1999). "Solution of fluid-structure interaction problems using a coupled finite element and variational boundary element technique". *Journal of the Acoustical Society of America*, Vol. 88, pp 2459 –2466.

- Bathe, K.J. Editor. (c1996). Finite element procedures. Englewood Cliffs, N.J.: *Prentice-Hall*.
- Cook, R.D., Malkus, D.S., Plesha, M.E. and Witt, R.J. (2002). "Concepts and applications of finite element analysis". 4th Ed., N.Y.: *John Wiley and Sons, Inc.*
- Brebbia, C.A., Telles, J.C. and Wrobel, L.C. (1984). Boundary element techniques. Berlin and New York.: *Springer Verlag*.
- Brebbia, C.A. (2006). Boundary elements XVIII. *Proceedings of the 28th International Conference on Boundary Element and other Mesh Reduction Methods*, Southampton and Boston: WIT Press.
- Rouquette, J., Haines, J., Bornand, V., Pintard, M, Papet, Ph., Bousquet, C., Konczewicz, L., Gorelli, F.A. and Hull, S. (2004). "Pressure tuning of the morphotropic phase boundary in piezoelectric lead zirconate titanate". *Phys. Rev. B*, Vol. 70, No. 1, pp 104-108.
- Liu, W., Jiang, B. and Zhu, W. (2000). "Self-biased dielectric bolometer from epitaxially grown $\text{Pb}(\text{Zr},\text{Ti})\text{O}_3$ and lanthanum-doped $\text{Pb}(\text{Zr},\text{Ti})\text{O}_3$ multilayered thin films". *Applied Physics Letters*, Vol. 77, No. 7, pp 1047–1049.